ISSN 0023-1584, Kinetics and Catalysis, 2007, Vol. 48, No. 6, pp. 853–863. © MAIK "Nauka/Interperiodica" (Russia), 2007.
Original Russian Text © M.Yu. Smirnov, D.Yu. Zemlyanov, E.I. Vovk, 2007, published in Kinetika i Kataliz, 2007, Vol. 48, No. 6, pp. 912–923.

MECHANISMS OF CATALYTIC REACTIONS

Mechanism of the Reaction NO + H_2 on the Pt(100)-hex Surface under Conditions of the Spatially Nonuniform Distribution of Reacting Species

M. Yu. Smirnov[a], D. Yu. Zemlyanov[b], and E. I. Vovk[a]

[a] *Boreskov Institute of Catalysis, Siberian Branch, Russian Academy of Sciences, Novosibirsk, 630090 Russia*
[b] *Purdue University, Birck Nanotechnology Center, West Lafayette, USA*
e-mail: smirnov@catalysis.ru

Received November 13, 2006

Abstract—The interaction of hydrogen with $NO_{ads}/1 \times 1$ islands produced by NO adsorption on the reconstructed surface Pt(100)-hex was studied by high-resolution electron energy loss spectroscopy (HREELS) and the temperature-programmed reaction (TPR) method. The islands are areas of the unreconstructed surface Pt(100)-1×1 saturated with NO_{ads} molecules. The hexagonal phase around these islands adsorbs much more hydrogen near room temperature than does the clean Pt(100)-hex surface. It is assumed that hydrogen is adsorbed on the hexagonal surface areas that are adjacent to, and are modified by, the $NO_{ads}/1 \times 1$ islands. The reaction of adsorbed hydrogen atoms with NO_{ads} takes place upon heating and has the character of so-called surface explosion. The TPR peaks of the products of this reaction—nitrogen and water—occur at T_{des} ~ 365–370 K, their full width at half-maximum being ~5–10 K. In the case of the $NO_{ads}/1 \times 1$ islands preactivated by heating in vacuo above the NO desorption onset temperature (375–425 K), after the admission of hydrogen at 300 K, the reaction proceeds in an autocatalytic regime and the product formation rate increases monotonically at its initial stage. In the case of activation at 375 K, during the initial, slow stage of the reaction (induction period), hydrogen reacts with nitric oxide molecules bound to structure defects (NO_{def}). After activation at 425 K, the induction period is characterized by the formation and consumption of imido species (NH_{ads}). It is assumed that NH_{ads} formation involves N_{ads} atoms that have resulted from NO_{ads} dissociation on defects upon thermal activation. The induction period is followed by a rapid stage of the reaction, during which hydrogen reacts with $NO_{1 \times 1}$ molecules adsorbed on 1×1 areas, irrespective of the activation temperature. After the completion of the reaction, the areas of the unreconstructed phase 1×1 are saturated with adsorbed hydrogen. The formation of H_{ads} is accompanied by the formation of a small amount of amino species (NH_{2ads}).

DOI: 10.1134/S0023158407060158

INTRODUCTION

The kinetics of heterogeneous catalytic reactions is conventionally described in terms of the law of coverage action [1], which is valid only for the uniform distribution of reacting species on the catalyst surface. However, even when the surface of a metal single crystal is used as the catalyst, the catalytic reaction often takes place in a chemically inhomogeneous adsorption layer. For example, for the reaction NO + H_2 on Pt(100), Rh(110), and other surfaces under certain conditions, photoemission electron microscopy (PEEM) with a space resolution of ~1 μm detected the propagation of surface waves due to the regular variation of the spatial distribution of the components of the adsorption layer [2–4]. Furthermore, it was demonstrated by field electron microscopy (FEM) and field ion microscopy (FIM) (space resolution of ~20 and ~3 Å, respectively) that catalytic reactions may be accompanied by the propagation of surface chemical waves [5].

One possible cause of the spatial chemical inhomogeneity of the adsorption layer on the catalyst surface is the adsorption-induced reconstruction of the surface. For example, NO adsorption on the reconstructed hexagonal surface Pt(100)-hex, which is more stable when clean, causes the back reconstruction of the surface [6, 7], yielding islands of the unreconstructed phase 1×1 saturated with NO_{ads} molecules [8]. Because of the significant difference between the atomic densities of the 1×1 and hex structures, the back reconstruction hex $\longrightarrow$ 1×1 forces part of the platinum atoms out of the surface into the overlying layer, yielding flat clusters of monoatomic height [9, 10]. Nitric oxide adsorbed on Pt(100)-hex can be in two molecular states: one is NO bound to 1×1 sites ($NO_{1 \times 1}$), and the other is NO occupying structure defects at the hex/1×1 boundary or on steps formed by clusters of expelled atoms (NO_{def}). The hexagonal phase surrounding the islands is almost free of adsorbed species.

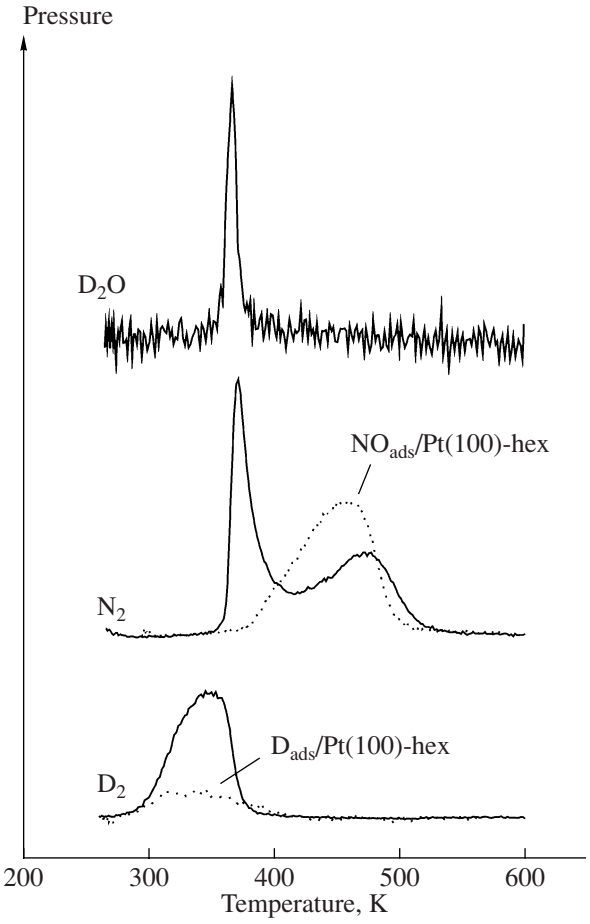

Fig. 1. Spectra of the TPR products—D_2, $^{15}N_2$, and D_2O—recorded after D_2 adsorption on the Pt(100)-hex surface containing NO_{ads} islands. The surface coverage is θ_{NO} = 0.2 ML; D_2 exposure, 20 L; T = 270 K; $P = 6 \times 10^{-8}$ mbar. The dashed lines are the D_2 desorption spectrum recorded after deuterium adsorption on the clean Pt(100)-hex surface under the same conditions and the spectrum of N_2 desorption from the 0.2-ML layer NO_{ads} on the Pt(100)-hex surface.

Hydrogen adsorption on Pt(100)-hex at low temperatures of ≤200 K is also accompanied by the back reconstruction hex ⟶ 1 × 1 [7, 11–13], yielding different H_{ads} states, including hydrogen occupying defect sites [14]. However, at $T \sim 300$ K, hydrogen is adsorbed only in insignificant amounts and its limiting concentration of $\sim 10^{14}$ (at H)/cm^2 is reached rapidly [13, 15]. According to low energy electron diffraction (LEED) data, the surface structure remains nearly hexagonal upon hydrogen adsorption [13, 15].

Titration of the $NO_{ads}/1 \times 1$ islands with hydrogen is a convenient means to study the mechanisms of catalytic reactions proceeding under conditions of the nonuniform distribution of reacting species on the surface. In our earlier works, we demonstrated that, after thermal activation in vacuo and cooling to room temperature, the $NO_{ads}/1 \times 1$ islands react with hydrogen to yield N_2 as the main N-containing product [16–18]. This reaction has an induction period, whose duration depends on the initial NO coverage of the surface [16] and the activation temperature [17]. Here, we present the results of a systematic mechanistic study of the interaction between hydrogen and $NO_{ads}/1 \times 1$ islands near room temperature. In this study, we used high-resolution electron energy loss spectroscopy (HREELS), which enables one to record the vibrational spectra of species in the adsorption layer, and the temperature-programmed reaction (TPR) method. Special attention was focused on the chemical nature of the adsorbed species involved in the reaction. The purpose of the study was to construct a model for the $NO_{ads}/1 \times 1 + H_2$ reaction occurring under conditions of the nonuniform distribution of reacting species on the catalyst surface.

EXPERIMENTAL

All experiments were carried out in the ultrahigh-vacuum chamber of a VG ADES 400 electron spectrometer (England) at a residual pressure of $\sim 2 \times 10^{-11}$ mbar. High-resolution electron energy loss spectra were obtained using an electron gun with an EMU50 monochromator and a 150° hemispherical electrostatic energy analyzer. The electron beam, incident at an angle of 35°, was in-specular-reflected from the surface of the single-crystal sample. For the ~2.5-eV kinetic energy of the electrons in the primary beam, the resolution was 65–80 cm^{-1} (8–10 meV). TPR spectra were recorded while heating the sample at a constant rate of 10 K/s using a VG QXK 400 mass spectrometer equipped with a double Re anode and a channeltron multiplier with an amplification factor of 10^8. The temperature regime and HREELS and TPR data acquisition were controlled using a purpose-designed controller and control software [19, 20].

We used platinum single crystals with one surface (100)-oriented with an error of <0.5°. The single crystal to be examined was secured between two tantalum wires by spot welding. The crystal could be heated up to 1200 K by passing electric current through the wires. The sample holder was in thermal contact with a vessel through which liquid nitrogen was passed to cool the crystal. The crystal temperature was measured with a chromel/alumel thermocouple welded to the side surface of the crystal. The Pt(100) surface was cleaned by Ar^+ sputtering and by heat treatment in oxygen and in vacuo. In TPR experiments, we used D_2 and ^{15}NO in order to reliably distinguish all reaction products.

RESULTS AND DISCUSSION

Coadsorption of NO and Hydrogen (Deuterium)

Only small amounts of hydrogen ($\sim 10^{14}$ (at H)/cm^2) can be adsorbed onto the clean reconstructed surface Pt(100)-hex at room temperature [13, 15]. However, it was found that the surface containing $NO_{ads}/1 \times 1$

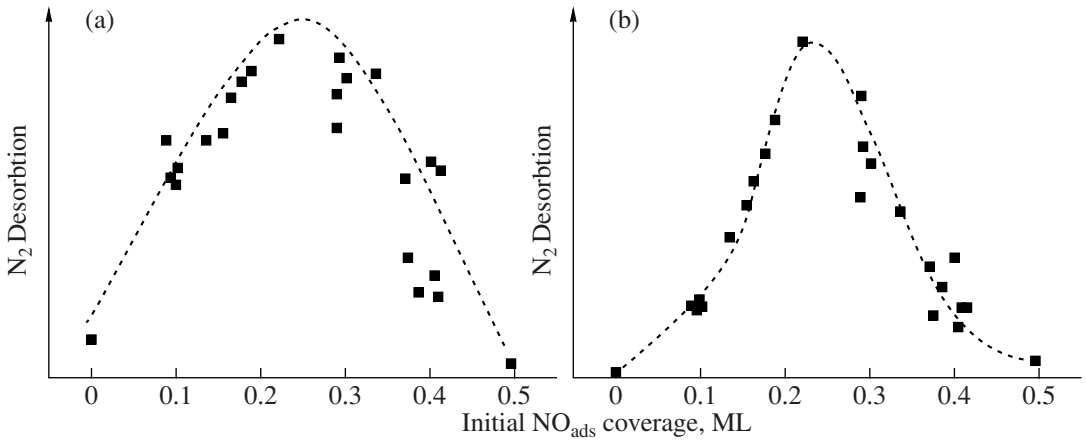

Fig. 2. Amounts of (a) desorbed D_2 and (b) resulting N_2 as a function of the initial NO_{ads} coverage of the Pt(100)-hex surface for the TPR in a mixed layer obtained by saturating the surface with deuterium. Deuterium adsorption conditions: 270 K, 6×10^{-8} mbar, 20 L.

islands is capable of adsorbing considerable amounts of hydrogen. Figure 1 shows the TPR spectrum recorded after 20 L[1] deuterium exposure at 270 K and a pressure of $D_2 = 6 \times 10^{-8}$ mbar onto a reconstructed surface containing 0.2 ML[2] of NO_{ads}. The main products detected by TPR were D_2, N_2, and D_2O. For comparison, Fig. 1 shows the D_2 desorption spectrum obtained for the clean reconstructed surface after deuterium adsorption under the same conditions, as well as the N_2 spectrum arising from NO_{ads} dissociation in the layer containing no adsorbed deuterium [21]. It is evident from these data that, in the presence of $NO_{ads}/1 \times 1$ islands, the amount of desorbed deuterium is several times larger. Furthermore, at $T > 350$ K, D_2 desorption gives way to the reaction between adsorbed deuterium and NO_{ads}, which yields N_2 and D_2O, which show themselves in the TPR spectrum as narrows peaks at 360 and 365 K, respectively. Both D_2 desorption and the identification of the products of the $D_{ads} + NO_{ads}$ reaction provide evidence that the $NO_{ads}/1 \times 1$ islands markedly increase the hydrogen adsorption capacity of the reconstructed surface Pt(100)-hex. The N_2 desorption spectrum of the mixed layer $D_{ads} + NO_{ads}$ additionally shows a broad peak at $T_{des} \sim 465$ K, which is likely due to the dissociation of NO_{ads} that is in excess over D_{ads}. Besides the products indicated in Fig. 1, small amounts of NO, N_2O, and O_2 are identified in the TPR spectrum. The way in which these products are released is consistent with the desorption of individual NO_{ads} formed on the Pt(100)-hex surface [21].

We studied the effect of the NO_{ads} coverage on the hydrogen (deuterium) adsorption capacity of the surface. Figure 2 shows how the amounts of adsorbed deuterium and of the nitrogen resulting from the reaction depend on the initial NO_{ads} coverage (θ^0_{NO}). Both curves pass through a maximum in the vicinity of $\theta^0_{NO} \approx 0.25$ ML. The surface saturated with NO_{ads} does not adsorb deuterium.

It can be assumed that, around the $NO_{ads}/1 \times 1$ islands, there are areas of the pure hexagonal phase whose structure is modified so that it can adsorb hydrogen under conditions ruling out hydrogen adsorption on the regular Pt(100)-hex surface. The reconstructive adsorption of NO on Pt(100)-hex is known to take place via the island nucleation and growth mechanism, so, starting at some low surface coverage, the NO_{ads} concentration increases owing to $NO_{ads}/1 \times 1$ islands growing in size rather than in number [9, 10]. Therefore, the nonmonotonic variation of the amount of adsorbed deuterium (Fig. 2) can be explained by the fact that, as θ^0_{NO} increases, the total area of the modified regions of the hexagonal surface capable of adsorbing hydrogen first increases and, after the critical value of the NO_{ads} coverage is reached, begins to decrease because of the overlap of these regions. In simplified form, the spatial distribution of adsorbed species in the $D_{ads} + NO_{ads}$ layer on the Pt(100)-hex surface as a function of the initial coverage θ^0_{NO} is illustrated in Fig. 3.

Thus, unlike the regular Pt(100)-hex surface, the surface having $NO_{ads}/1 \times 1$ islands adsorbs hydrogen (deuterium) rather readily to form a stable $D_{ads} + NO_{ads}$ adsorption layer. Hydrogen is believed to occupy limited areas of the hexagonal surface around the $NO_{ads}/1 \times 1$ islands. The TPR between adsorbed NO and hydrogen is initiated by heating to ≥350 K and yields N_2 and D_2O, which show themselves as narrow

[1] 1 L = 1 Langmuir = 1.3×10^{-6} mbar s.

[2] 1 ML = 1 monolayer, which is a relative surface coverage unit. In this study, 1 monolayer is taken to be the concentration of adsorbed molecules equal to the number of platinum atoms on 1 cm^2 of the Pt(100)-1 × 1 surface; that is, 1 ML = 1.28×10^{15} cm^{-2}.

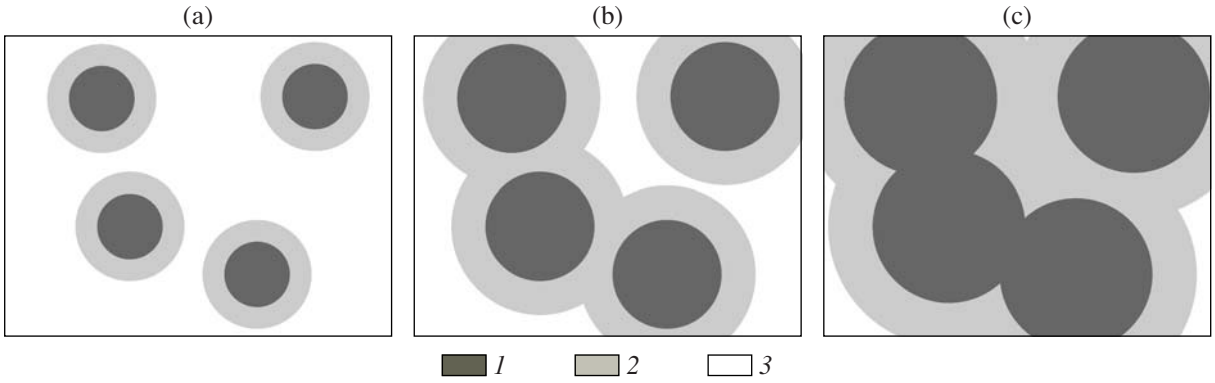

Fig. 3. Model of the $NO_{ads} + D_{ads}$ layer forming on the Pt(100)-hex surface at (a) low, (b) medium, and (c) high initial coverages (θ_{NO}): (*1*) unreconstructed phase areas occupied by NO_{ads}, (*2*) modified hexagonal surface areas adsorbing hydrogen, and (*3*) clean hexagonal surface.

desorption peaks. This phenomenon was given the name of surface explosion [22].

Reaction between Hydrogen and Activated $NO_{ads}/1 \times 1$ Islands

Earlier, we demonstrated that the locally saturated $NO_{ads}/1 \times 1$ islands formed by NO adsorption on the Pt(100)-hex surface do not enter into the titration reaction with hydrogen near room temperature even when they occupy only part of the surface [16]. The nonreactivity of the islands cannot be due to the impossibility of hydrogen adsorption on the reconstructed phase. Indeed, it was demonstrated above that, in the presence of phase 1×1 islands saturated with adsorbed NO on the Pt(100)-hex surface, part of the hexagonal phase around the islands acquires the capacity for adsorbing considerable amounts of hydrogen. The nonreactivity of the saturated $NO_{ads}/1 \times 1$ islands toward hydrogen is likely due to the absence of empty adsorption sites in the areas of the unreconstructed phase. The absence of empty sites in the islands prevents NO_{ads} dissociation, the key step of the reaction. Nevertheless, the reaction will be possible if, before the admission of hydrogen, the islands are activated by heating to ≥370 K in vacuo. NO_{ads} desorption accompanied by the dissociation of part of the adsorbed molecules begins under these conditions [16–18, 21, 23].

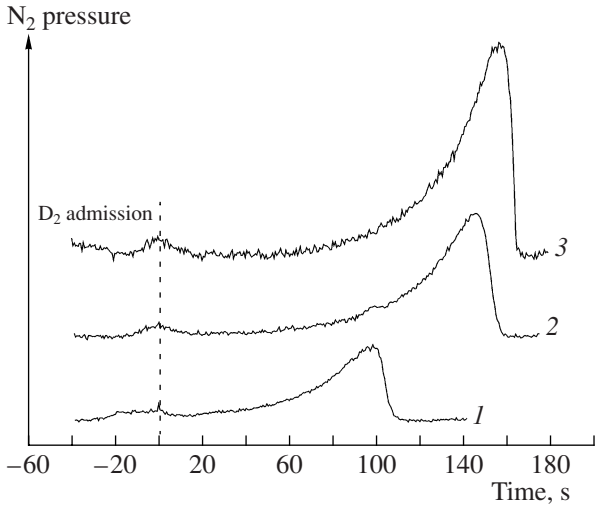

Fig. 4. $^{15}N_2$ formation under isothermal conditions by the interaction of activated $^{15}NO_{ads}/1 \times 1$ islands with deuterium at 300 K, a D_2 pressure of 4×10^{-8} mbar, and an initial coverage of θ^0_{NO} = (*1*) 0.20, (*2*) 0.35, and (*3*) 0.50 ML. The islands were activated by heating in vacuo at 375 K.

Hydrogen admission at 300 K onto the reconstructed surface with $NO_{ads}/1 \times 1$ islands activated at 375 K results in nitrogen formation (Fig. 4). The shape of the nitrogen formation curves is independent of the initial coverage θ^0_{NO}. The release of N_2 into the gas phase is preceded by an induction period, whose duration increases with increasing θ^0_{NO}. The reaction is autoaccelerated during the induction period. As a consequence, the nitrogen formation rate peaks and then falls off sharply to zero. The cause of the autocatalytic behavior of the reaction is clear from the overall equation

$$2NO_{ads} + 2H_2 \longrightarrow N_2 + 2H_2O + 2*,$$

where * is an empty site in an area with the 1×1 structure. It follows from this equation that, as the titration reaction proceeds, the concentration of empty sites involved in the key step of the reaction (NO_{ads} dissociation) increases. TPR spectra indicate that, after the reaction is complete, the surface is largely covered with adsorbed hydrogen. Earlier, we found that the titration of the $NO_{ads}/1 \times 1$ islands with hydrogen at 300 K leads to the complete replacement of NO_{ads} with H_{ads} on unreconstructed surface areas, but hydrogen adsorption does not propagate to the reconstructed surface areas surrounding the 1×1 phase islands [24].

The changes taking place in the adsorption layer during the titration of the $NO_{ads}/1 \times 1$ islands with deuterium at 300 K and $P_{D_2} \sim 10^{-10}$ mbar were studied by HREELS (Fig. 5). The islands were preactivated by heating in vacuo at 375 K. The spectra were recorded in the presence of deuterium. Near each spectrum, we indicate the time when the spectrum registration is completed (counted from the D_2 admission instant). Initially, before the reaction, two states of NO_{ads} are present in the activated islands, namely, NO adsorbed on 1×1 areas ($NO_{1\times1}$, $\nu(NO) = 1600$ cm^{-1}) and NO adsorbed on defects (NO_{def}, $\nu(NO) = 1775$ cm^{-1}) [8, 17, 18, 23, 25].

The spectra presented in Fig. 5 suggest that the NO_{ads} states disappear successively during the reaction, first NO_{def} and then $NO_{1\times1}$. The way the intensity of the $\nu(NO)$ band due to $NO_{1\times1}$ varies with time (see the inset in Fig. 5) is consistent with the induction period of N_2 formation (Fig. 4). The induction period is followed by a dramatic weakening of the $\nu(NO)$ band because of $NO_{1\times1}$ consumption. Simultaneously, the band shifts from 1600 to 1565 cm^{-1}. This shift is conventionally attributed to the weakening of the dipole–dipole interaction in the system of identical oscillators. In turn, this weakening is due to the decrease in the local concentration of $NO_{1\times1}$ molecules [26, 27]. After the reaction is complete, the electron energy loss spectrum does not show any bands characteristic of adsorbed NO and shows a weak new band at 1080 cm^{-1}. This band is due to the bending vibrations $\delta(ND_2)$ of adsorbed amino species, which form in small amounts (~0.02 ML) at the final stage of the reaction, when there are excess D_{ads} atoms on the 1×1 areas. The amino species were obtained on the unreconstructed surface Pt(100)-1×1 by titration of the adsorbed hydrogen layer with NO at 300 K. Earlier, we described the vibrational spectrum of NH_{2ads} on the Pt(100) surface [28] and the chemical properties of this species [29].

Figure 6 presents the series of electron energy loss spectra recorded during the reaction between hydrogen and $NO_{ads}/1 \times 1$ islands activated at a higher temperature of 425 K. The reaction was conducted at 300 K and a hydrogen pressure of ~10^{-10} mbar. Because all of the NO_{def} molecules were desorbed or dissociated upon heating to 425 K, the islands in their initial state contained only $NO_{1\times1}$ molecules, which are characterized by bands at 1600 and 360 cm^{-1}, and adsorbed oxygen atoms, which give rise to a $\nu(PtO)$ stretching band at 530 cm^{-1} in the electron energy loss spectrum.

After the admission of hydrogen, O_{ads} is the first to react and is consumed rapidly. Although NO_{def} is absent, the reaction again has an induction period, during which the intensity of the stretching band $\nu(NO)$ changes insignificantly (see the inset in Fig. 6). It is clear from Fig. 6 that, during the induction period, three electron energy loss bands at 930, 470, and 210 cm^{-1} first appear and then vanish. Another, very weak band

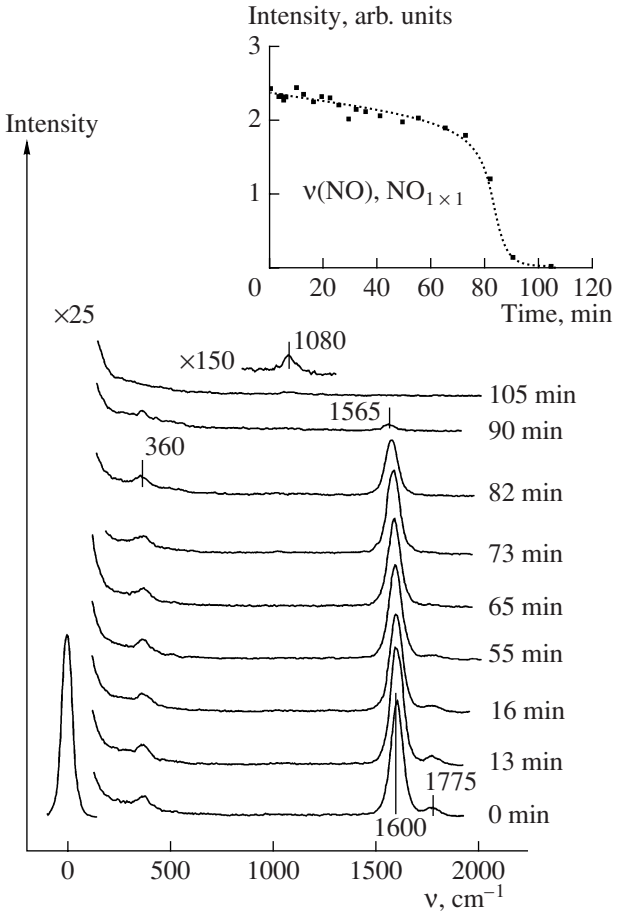

Fig. 5. Series of electron energy loss spectra recorded during the interaction of activated $NO_{ads}/1 \times 1$ islands with deuterium at 300 K and a D_2 pressure of ~10^{-10} mbar. The islands were activated by heating in vacuo at 375 K. Inset: intensity of the $\nu(NO)$ band for the $NO_{1\times1}$ state as a function of the D_2 exposure time.

was observed at a high frequency of 3185 cm^{-1} (not shown). The variation of the intensity of the strongest (930 cm^{-1}) band is illustrated in the inset in Fig. 6. After the disappearance of the bands considered, a rapid stage of the reaction begins, in which $NO_{1\times1}$, the main state of adsorbed NO, is consumed. After the reaction is complete, a small amount of amino species is observed on the surface. These species give rise to a weak $\delta(NH_2)$ band at 1450 cm^{-1} [28]. In the TPR spectrum recorded after the completion of the reaction, the main component is hydrogen, which is evidence of the occupation of the unreconstructed surface by H_{ads} atoms. Furthermore, the spectrum indicates the desorption of small amounts of nitrogen, which results from NH_{2ads} dissociation.

Obviously, the bands at 3185, 930, 470, and 210 cm^{-1} are due to an intermediate in the reaction between NO_{ads} and hydrogen that is formed and consumed within the induction period. Since the high-fre-

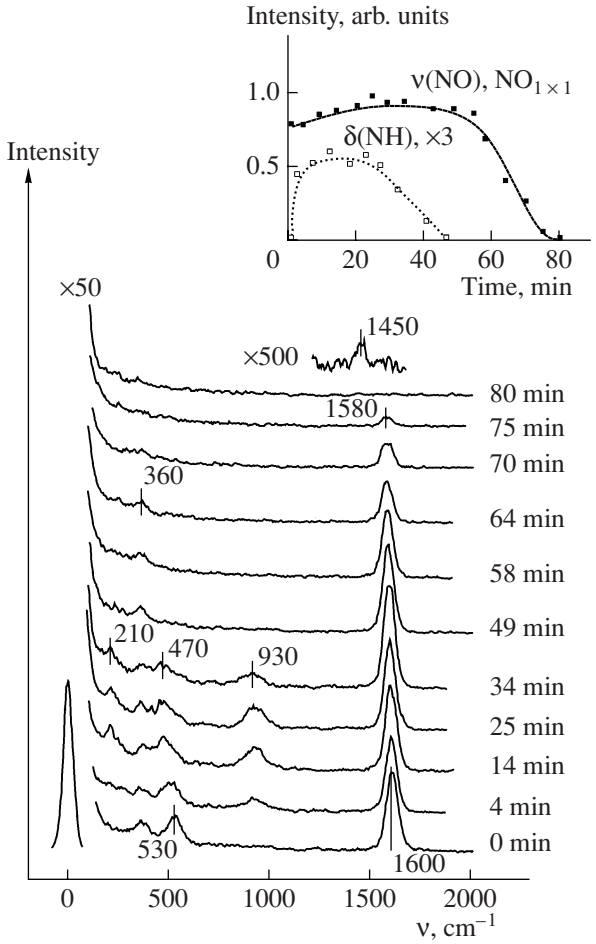

Fig. 6. Series of electron energy loss spectra recorded during the interaction of activated $NO_{ads}/1 \times 1$ islands with hydrogen at 300 K and an H_2 pressure of ~10^{-10} mbar. The islands were activated by heating in vacuo at 425 K. Inset: intensities of the ν(NO) band for the $NO_{1 \times 1}$ state and of the δ(NH) band for the NH_{ads} species as a function of the H_2 exposure time.

quency band at 3185 cm^{-1} falls in the region of the stretching vibrations of N–H bonds, it can be assumed that this intermediate is an NH_x species. In order to identify this species, we reacted $NO_{ads}/1 \times 1$ with H_2, D_2, and an $H_2 + D_2$ (1 : 1) mixture. The electron energy loss spectra recorded at the instant the maximum intermediate concentration is reached are presented in Fig. 7. Replacing H_2 with D_2 shifts the 930 cm^{-1} band to 690 cm^{-1}; therefore, hydrogen atoms are involved in the vibrations giving rise to this band. Note that this spectral region accommodates the N–H bending bands. The bands at 470 and 210 cm^{-1} do not change their place upon the replacement of H_2 with D_2. Obviously, the reaction involving the $H_2 + D_2$ mixture must yield a mixture of NH_yD_{x-y} ($x \le 3$, $y \le x$) intermediates. The spectrum observed for the isotopic mixture shows two bands in the region of N–H bending vibrations. Their frequencies are precisely equal to the frequencies observed for the reactions with H_2 (930 cm^{-1}) and D_2 (690 cm^{-1}). Observation of the two bands is possible only in the case of the formation of a mixture of the imido species NH_{ads} and ND_{ads}. These bands should be assigned to the bending vibrations δ(NH) and δ(ND), respectively. In the similar case of amino species resulting from the reaction between the $H_{ads} + D_{ads}$ mixture with NO on the Pt(100)-1 × 1 surface, the region of bending vibrations exhibits three bands, namely, $\delta(NH_2)$, δ(NHD), and $\delta(ND_2)$, which are due to NH_{2ads}, NHD_{ads}, and ND_{2ads}, respectively [28]. In the case of $NH_3 + ND_3$ adsorption on Fe(110), four bands due to the umbrella vibrations $\delta(NH_3)$, $\delta(NH_2D)$, $\delta(NHD_2)$, and $\delta(ND_3)$ were observed in the vibrational spectrum [30], whence it was deduced that ammonia is adsorbed in molecular form on this surface. The other bands in the spectrum of NH_{ads} (ND_{ads}), observed at 470 and 210 cm^{-1}, were assigned by us to the vibrations of the species as a whole perpendicular to the surface (ν(Pt–NH)) and parallel to the surface ($T_{x,y}$). The assignment of the vibrational bands of the NH_{ads} and ND_{ads} intermediates resulting from the $NO_{ads} + H_2$ (D_2) reaction on the Pt(100) surface is presented in Table 1. In Table 2, we compare NH_{ads} vibration frequencies on Pt(100) and on other metal surfaces.

Presumably, NH_{ads} can result from the hydrogenation of the nitrogen atoms (N_{ads}) that have formed by the dissociation of NO_{def} along the boundaries of the $NO_{ads}/1 \times 1$ islands upon heating to 425 K. The localization of NH_{ads} on structure defects is indicated by the fact that the electron energy loss spectrum of this species shows four bands. Indeed, the selection rules for in-specular-reflection HREELS allow only totally symmetrical vibrations characterized by a nonzero dynamic dipole moment perpendicular to the surface [48].

Table 1. Assignment of the vibrational bands of the imido species resulting from the interaction between hydrogen and $NO_{ads}/1 \times 1$ islands preactivated by heating at 425 K in vacuo

Adsorbed species	$T_{x,y}$, 210 cm^{-1}	ν(Pt–N), 470 cm^{-1}	δ(NH), 930 cm^{-1}	δ(ND), 690 cm^{-1}	δ(NH), 3185 cm^{-1}	δ(ND), cm^{-1}
NH_{ads}	+	+	+	–	+	–
ND_{ads}	+	+	–	+	–	–
$NH_{ads} + ND_{ads}$	+	+	+	+	–	–

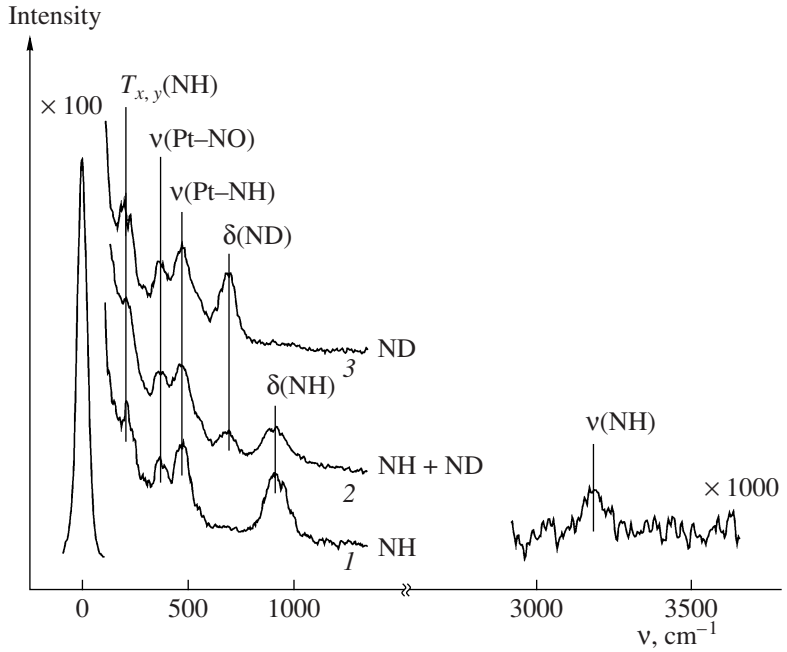

Fig. 7. Series of electron energy loss spectra recorded during the interaction of H_2 (*1*), D_2 (*2*), and an $H_2 + D_2$ (1 : 1) mixture (*3*), with $NO_{ads}/1 \times 1$ islands activated at 425 K at the instant of the maximum accumulation of imido species. The reaction temperature is 300 K.

Accordingly, for the NH_{ads} molecule on a flat surface, such as the interior of a 1×1 island, the spectrum is expected to contain two resolved bands, namely, ν(Pt–NH) and ν(NH), for the normal orientation of the molecule relative to the surface and three bands, namely, ν(Pt–NH), δ(NH), and ν(NH), for a tilted orientation of the molecule (Fig. 8). If NH is bound to a structure defect, such as a step, the symmetry of the adsorption complex will be reduced and extra vibrational modes will be allowed. An example is the vibration of the NH species as a whole in the direction normal to the step (Fig. 8).

Reaction of Hydrogen with Oxygen Atoms of the $NO_{ads}/1 \times 1$ Islands

As is demonstrated in Fig. 6, the oxygen atoms resulting from the activation of $NO_{ads}/1 \times 1$ islands at 425 K react readily with hydrogen at 300 K and are consumed first. This is consistent with the view that O_{ads} is highly reactive toward hydrogen on Pt(100) and

Table 2. Vibration frequencies of NH species adsorbed on metal surfaces (the numbers in parentheses are the vibration frequencies of ND_{ads})

Surface	ν(M–NH)	δ(NH), cm^{-1}	ν(NH), cm^{-1}	Reference
Pt(100)-hex	470 (470)	930 (690)	3185	This work
Ni(110)	400	–	3240 (2410)	[31, 32]
Ni(111)	620 (580)	1270 (950)	3340 (2480)	[33]
Cu(110)	400–430	760–780	3240–3270	[34–36]
Cu(111)	610	1100	3350	[37]
Ru(001)	570–690 (570–680)	1350 (1060)	3310–3370 (2455)	[38–42]
Ru($10\bar{1}0$)	690	–	3290	[43]
Ru($11\bar{2}0$)	600 (570)	670–710 (475–515)	3305 (2410)	[44]
Pt(111)	490	1390–1410	3280–3320	[45–47]

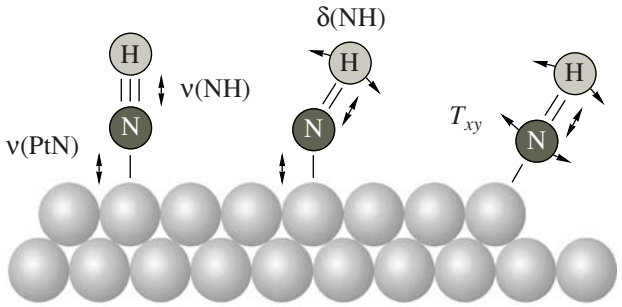

Fig. 8. Different orientations of adsorbed imido species and vibrations allowed for in-specular-reflection HREELS.

other platinum surfaces [49]. It was mentioned above that, as the NO_{ads} layer is heated in vacuo, the NO molecules bound to structure defects (NO_{def}), many of which are located at the boundaries between the islands and the hexagonal phase, are the first to undergo desorption and dissociation. There is good reason to assume that the oxygen atoms resulting from NO_{def} dissociation are also located at the island boundaries. Here, the following question arises: What behavior will be shown by oxygen atoms located in the interior of an $NO_{ads}/1 \times 1$ island?

In order to answer this question, we prepared an adsorption layer consisting of NO_{ads} and O_{ads} on the reconstructed surface in the following way (Fig. 9). Initially, NO was adsorbed onto the surface up to a coverage of 0.2 ML. This produced $NO_{ads}/1 \times 1$ islands, and a considerable part of the surface remained reconstructed (this state of the surface is described by spectrum *1* in Fig. 9). Next, the islands were activated by heating to 400 K. This treatment removed the NO_{def} molecules and produced oxygen atoms (see the band at 530 cm^{-1}). Additional NO adsorption caused an increase in θ_{NO} owing to the reoccupation of those adsorption sites in the initial islands that had become vacant as a result of activation and owing to the growth of the islands. As judged from the electron energy loss spectrum, NO_{def} molecules reappear in the adsorption layer and are located at the new boundaries between the islands and the hexagonal phase. It follows from spectrum *4* in Fig. 9 that, after the surface is exposed to 5.5 L H_2 at room temperature, the intensity of the ν(PtO) band remains unchanged. Therefore, the adsorbed oxygen atoms in the islands thus prepared do not react with hydrogen.

When thermal activation at 400 K is repeated, the NO_{def} molecules disappear again, while the O_{ads} concentration increases. The adsorption layer becomes active. The reaction of this layer with hydrogen at 300 K has the same specific features as were noted above (Fig. 10): there is an induction period during which the intensity of the ν(NO) band of $NO_{1\times1}$ is approximately constant, and the formation and consumption of NH_{ads} take place. The induction period is

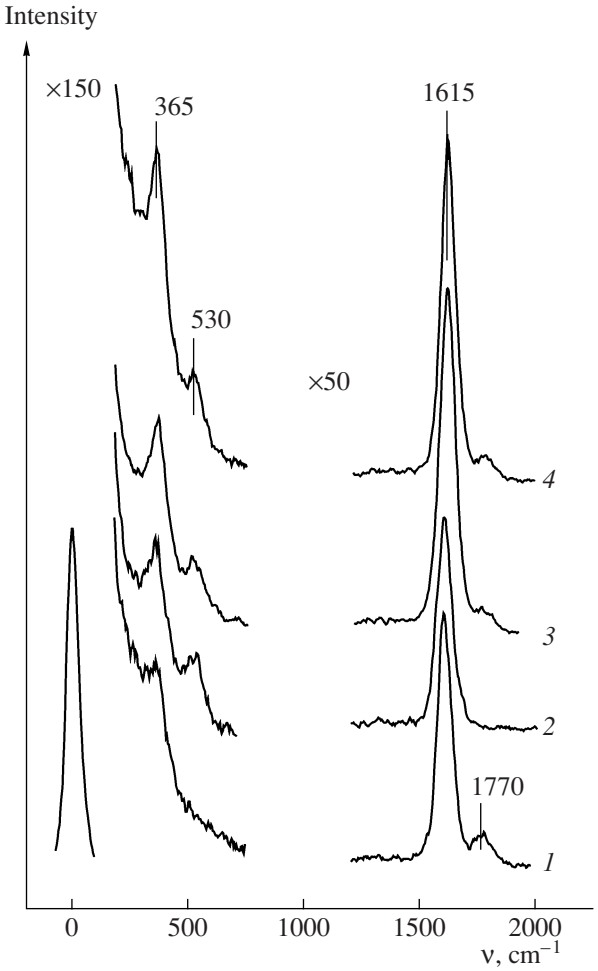

Fig. 9. Electron energy loss spectra recorded successively (*1*) after 2 L NO adsorption at 300 K on the Pt(100)-hex surface, (*2*) after heating the NO_{ads} layer in vacuo at 400 K, (*3*) after the additional adsorption of 1 L NO at 300 K, and (*4*) after 5.5 L hydrogen exposure at 300 K.

followed by a rapid reaction stage in which $NO_{1\times1}$ is consumed. After the reaction, the 1×1 areas are saturated with adsorbed hydrogen. However, in this case, the participation of oxygen atoms in the reaction has a significant distinctive feature, as is clear from a comparison between Figs. 9 and 10. While the ν(PtO) band in Fig. 9 disappears at the very onset of the reaction, the same band in Fig. 10 persists up to the end of the induction period, although its intensity decreases. For the sake of convincingness, we present the spectra recorded in the low-frequency region at the instant of the highest NH_{ads} concentration for once- and twice-activated $NO_{ads}/1 \times 1$ islands (Fig. 11, curves *2*, *3*, respectively). Figure 11 also shows the spectrum of the activated NO_{ads} layer containing $NO_{1\times1}$ and O_{ads} (curve *1*). This spectrum indicates the precise positions of the stretching bands ν(Pt–NO) and ν(PtO) (470 and 530 cm^{-1}, respectively). A comparison between the three spectra presented in Fig. 11 suggests that O_{ads} is indeed present

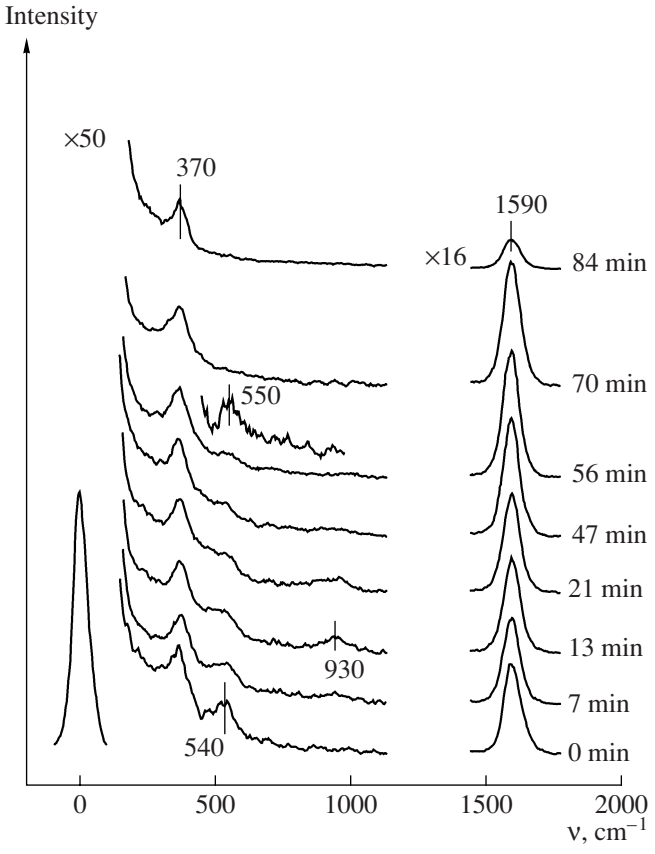

Fig. 10. Series of electron energy loss spectra recorded during the interaction of hydrogen with $NO_{ads}/1 \times 1$ islands obtained as described in Fig. 9 and additionally activated by heating in vacuo at 400 K. The reaction with hydrogen was conducted at 300 K.

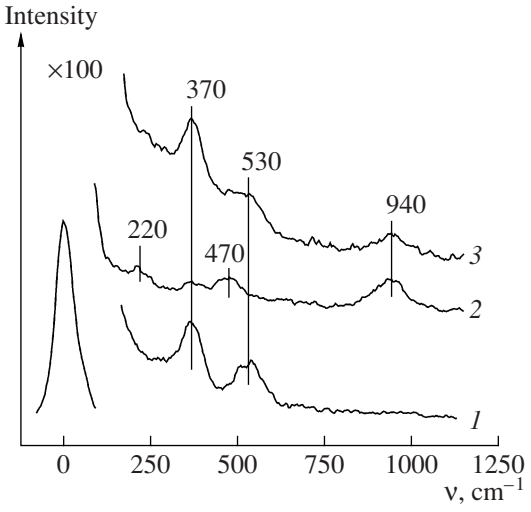

Fig. 11. Comparison of electron energy loss spectra recorded (*1*) for the NO_{ads} layer activated by heating in vacuo at 425 K on the Pt(100)-hex surface, (*2*) during the interaction of hydrogen with $NO_{ads}/1 \times 1$ activated at 425 K, and (*3*) during the interaction of hydrogen with $NO_{ads}/1 \times 1$ islands twice activated at 400 K.

in the adsorption layer during the titration of the twice-activated $NO_{ads}/1 \times 1$ islands at the instant the amount of NH_{ads} reaches its maximum.

To explain the changes observed in the electron energy loss spectra, we suggest the following scenario for the formation and activation of $NO_{ads}/1 \times 1$ islands and their subsequent reaction with hydrogen (Fig. 12). The unsaturated NO_{ads} adsorption layer is formed by comparably small $NO_{ads}/1 \times 1$ islands locally saturated with nitric oxide molecules in the $NO_{1 \times 1}$ and NO_{def} states. An example of such an island is schematically shown in Fig. 12a. It is assumed that the NO_{def} molecules occupy defect sites at the boundaries between the islands and the reconstructed hexagonal phase. Thermal activation causes desorption of part of the NO molecules, mainly NO_{def}. As a result, the dissociation of other NO_{def} molecules on the defect sites is initiated, yielding O_{ads} (Fig. 12b). Reexposure to NO causes the islands to grow, and the adsorbed oxygen atoms find themselves blocked by NO_{ads} molecules inside the islands (Fig. 12c). The boundaries between the extended islands and the hexagonal phase are occupied by NO_{def} molecules. Upon the reactivation of the adsorption layer, these molecules generate O_{ads} atoms (Fig. 12d).

With this distribution of adsorbed species in the island (Fig. 12d), when part of the O_{ads} atoms is in the interior of the island and part is at the boundary between the island and the hexagonal phase, the reaction with hydrogen at 300 K can be represented in the following way. Initially, hydrogen is adsorbed on modified hexagonal surface areas around the islands (Fig. 12e). The resulting H_{ads} atoms move toward the island boundary, where they react with O_{ads}. Next, during the induction period, H_2 reacts with NO_{def} molecules and N_{ads} atoms located at the island boundary (Fig. 12f). After the induction period, the reaction zone propagates throughout the island interior, where hydrogen reacts with $NO_{1 \times 1}$ and O_{ads} (Fig. 12g). The reaction ends in the complete consumption of adsorbed nitric oxide and oxygen and in the occupation of the 1×1 areas by hydrogen (Fig. 12h).

CONCLUSIONS

(1) A multifold increase in the hydrogen sorption capacity of the hexagonal phase takes place in the presence of 1×1 phase islands saturated with NO molecules on the reconstructed surface. In all likelihood, hydrogen is adsorbed on limited hexagonal phase areas around $NO_{ads}/1 \times 1$ islands.

(2) The reaction between adsorbed NO and hydrogen at 300 K takes place on unreconstructed phase areas of the Pt(100) surface only when there are empty sites for NO dissociation and hydrogen adsorption. Empty sites can be produced by preheating the

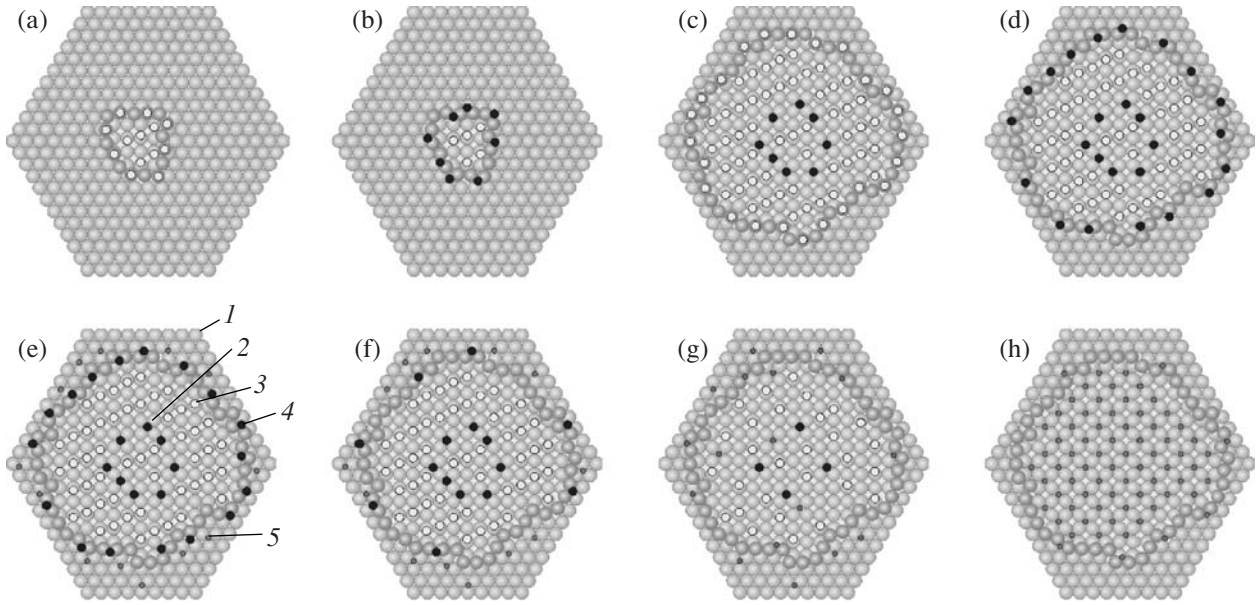

Fig. 12. Schematic representation of the formation and activation of $NO_{ads}/1 \times 1$ islands on the Pt(100)-hex surface and of their interaction with hydrogen: (a) small NO_{ads} islands before activation; (b) activation of the islands by heating in vacuo; (c) adsorption of extra NO; (d) reactivation of the islands; (e) hydrogen adsorption on the modified part of the hexagonal surface around the $NO_{ads}/1 \times 1$ islands; (f) reaction between H_{ads} and O_{ads} at the boundary of an island; (g) penetration of H_{ads} into the interior of the island, where it reacts with $NO_{1 \times 1}$ and O_{ads}; (h) completion of the reaction between hydrogen and the $NO_{ads}/1 \times 1$ island, resulting in the formation of a saturated $H_{ads}/1 \times 1$ island; (*1*, *2*) Pt atoms in the regular structure; (*3*) NO_{ads}; (*4*) O_{ads}; (*5*) H_{ads}.

$NO_{ads}/1 \times 1$ islands in vacuo. The reaction between hydrogen and the activated islands proceeds in two steps. In the initial, slow step (induction period), hydrogen reacts with NO_{def} molecules and other species adsorbed on defects at boundaries of the islands. The slow step is followed by a rapid step, in which the reaction zone propagates throughout the surface of the unreconstructed phase and the $NO_{1 \times 1}$ molecules, bound to unreconstructed phase areas, get involved in the reaction.

(3) Under certain conditions, imido species form and are consumed during the induction period. It is most likely that the imido species are bound to defects at the island boundaries. The electron energy loss spectrum of the species shows bands at 3185, 930, 470, and 210 cm^{-1}, which were assigned to the ν(NH), δ(NH), ν(Pt–NH), and $T_{x,y}$ vibrations, respectively.

REFERENCES

1. Boreskov, G.K., *Geterogennyi kataliz* (Heterogeneous Catalysis), Moscow: Nauka, 1986.
2. Imbihl, R. and Ertl, G., *Chem. Rev.*, 1995, vol. 95, p. 697.
3. Mertens, F. and Imbihl, R., *Nature*, 1994, vol. 370, p. 124.
4. Slin'ko, M.M. and Jaeger, N.I., *Oscillating Heterogeneous Catalytic Systems*, Amsterdam: Elsevier, 1994, vol. 86.
5. Gorodetskii, V.V., *Doctoral (Chem.) Dissertation*, Novosibirsk: Inst. of Catalysis, 2001.
6. Bonzel, H.P., Broden, G., and Pirug, G., *J. Catal.*, 1978, vol. 53, p. 96.
7. Norton, P.R., Davies, J.A., Creber, D.K., Sitter, C.W., and Jackman, T.E., *Surf. Sci.*, 1981, vol. 108, p. 205.
8. Gardner, P., Tushaus, M., Martin, R., and Bradshaw, A.M., *Surf. Sci.*, 1990, vol. 240, p. 112.
9. Ritter, E., Behm, R.J., Potschke, G., and Wintterlin, J., *Surf. Sci.*, 1987, vol. 181, p. 403.
10. Hosler, W., Ritter, E., and Behm, R.J., *Ber. Bunsen-Ges. Phys. Chem.*, 1986, vol. 90, p. 205.
11. Pennemann, B., Oster, K., and Wandelt, K., *Surf. Sci.*, 1991, vol. 249, p. 35.
12. Radnik, J., Gitmans, F., Penneman, B., Oster, K., and Wandelt, K., *Surf. Sci.*, 1993, vols. 287–288, p. 330.
13. Klotzer, B. and Bechtold, E., *Surf. Sci.*, 1993, vol. 295, p. 374.
14. Zemlyanov, D.Yu., Smirnov, M.Yu., and Gorodetskii, V.V., *Catal. Lett.*, 1997, vol. 43, p. 181.
15. Barteau, M.A., Ko, E.I., and Madix, R.J., *Surf. Sci.*, 1981, vol. 102, p. 99.
16. Zemlyanov, D.Yu., Smirnov, M.Yu., and Gorodetskii, V.V., *Phys. Low-Dim. Struct.*, 1994, vols. 4–5, p. 89.
17. Zemlyanov, D.Yu., Smirnov, M.Yu., and Gorodetskii, V.V., *Catal. Lett.*, 1994, vol. 28, p. 153.
18. Zemlyanov, D.Yu., Smirnov, M.Yu., Gorodetskii, V.V., and Block, J.H., *Surf. Sci.*, 1995, vol. 329, p. 61.
19. Kaichev, V.V., Sorokin, A.M., Boronin, V.A., and Badalyan, A.M., *Avtometriya*, 1997, no. 5, p. 15.

20. Kaichev, V.V., Sorokin, A.M., Badalyan, A.M., Nikitin, D.Yu., and Moskovkin, O.V., *Prib. Tekh. Eksp.*, 1997, vol. 40, p. 575.
21. Zemlyanov, D.Yu., Smirnov, M.Yu., and Gorodetskii, V.V., *React. Kinet. Catal. Lett.*, 1994, vol. 53, p. 87.
22. Lesley, M.V. and Schmidt, L.D., *Surf. Sci.*, 1985, vol. 155, p. 215.
23. Zemlyanov, D.Yu. and Smirnov, M.Yu., *React. Kinet. Catal. Lett.*, 1994, vol. 53, p. 97.
24. Zemlyanov, D.Yu., Smirnov, M.Yu., and Vovk, E.I., *Langmuir*, 1999, vol. 15, p. 135.
25. Pirug, G., Bonzel, H.P., Hopster, H., and Ibach, H., *J. Chem. Phys.*, 1979, vol. 71, p. 593.
26. Hollins, P. and Pritchard, J., *Prog. Surf. Sci.*, 1985, vol. 19, p. 275.
27. Smirnov, M.Yu., Zemlyanov, D.Yu., Gorodetskii, V.V., and Vovk, E.I., *Surf. Sci.*, 1998, vol. 414, p. 409.
28. Zemlyanov, D.Yu., Smirnov, M.Yu., and Gorodetskii, V.V., *Surf. Sci.*, 1997, vol. 391, p. 37.
29. Smirnov, M.Yu. and Zemlyanov, D., *J. Phys. Chem. B*, 2000, vol. 104, p. 4661.
30. Erley, W. and Ibach, H., *Surf. Sci.*, 1982, vol. 119, p. L357.
31. Bassignana, I.C., Wagemann, K., Kuppers, J., and Ertl, G., *Surf. Sci.*, 1986, vol. 175, p. 22.
32. Takehiro, N., Mukai, K., and Tanaka, K., *J. Chem. Phys.*, 1995, vol. 103, p. 1650.
33. Gland, J.L., Fisher, G.B., and Mitchell, G.E., *Chem. Phys. Lett.*, 1985, vol. 119, p. 89.
34. Carley, A.F., Davies, P.R., Roberts, M.W., and Vincent, D., *Top. Catal.*, 1994, vol. 1, p. 35.
35. Afsin, B., Davies, P.R., Pashutsky, A., Roberts, M.W., and Vincent, D., *Surf. Sci.*, 1993, vol. 284, p. 109.
36. Afsin, B., Davies, P.R., Pashutsky, A., and Roberts, M.W., *Surf. Sci.*, 1991, vol. 259, p. L724.
37. Boronin, A., Pashutsky, A., and Roberts, M.W., *Catal. Lett.*, 1992, vol. 16, p. 345.
38. Dietrich, H., Jacobi, K., and Ertl, G., *Surf. Sci.*, 1997, vol. 377-379, p. 308.
39. Dietrich, H., Jacobi, K., and Ertl, G., *J. Chem. Phys.*, 1996, vol. 105, p. 8944.
40. Parmeter, J.E., Schwalke, U., and Weinberg, W.H., *J. Am. Chem. Soc.*, 1988, vol. 110, p. 53.
41. Rauscher, H., Kostov, K.L., and Menzel, D., *Chem. Phys.*, 1993, vol. 177, p. 473.
42. Shi, H., Jacobi, K., and Ertl, G., *J. Chem. Phys.*, 1995, vol. 102, p. 1432.
43. Dietrich, H., Jacobi, K., and Ertl, G., *J. Chem. Phys.*, 1997, vol. 106, p. 9313.
44. Wang, Y. and Jacobi, K., *Surf. Sci.*, 2002, vol. 513, p. 83.
45. Mieher, W.D. and Ho, W., *Surf. Sci.*, 1995, vol. 322, p. 151.
46. Sun, Y.-M., Sloan, D., Ihm, H., and White, J.M., *J. Vac. Sci. Technol., A*, 1996, vol. 14, p. 1516.
47. Herceg, E., Mudiyanselage, K., and Trenary, M., *J. Phys. Chem. B*, 2005, vol. 109, p. 2828.
48. Ibach, H. and Mills, D.L., *Electron Energy Loss Spectroscopy and Surface Vibrations*, New York: Academic, 1982.
49. Sobyanin, V.A., Boreskov, G.K., and Cholach, A.R., *Dokl. Akad. Nauk SSSR*, 1984, vol. 278, p. 1422.